Int J Adv Manuf Technol (1998) 14:656–663

The International Journal of Advanced Manufacturing Technology

Error Modelling and Measurement for the Rotary Table of Five-axis Machine Tools

Suk-Hwan Suh*, Eung-Suk Lee‡ and Se-Yong Jung*

*Computer Automated Manufacturing Laboratory, Department of Industrial Engineering, POSTECH, Pohang, 784; and ‡Automation Division, Research Institute of Industrial Science and Technology, Pohang, 784 Korea

Rotary tables are widely used with multi-axis machine tools as a means for providing rotational motions for the cutting tools on the three-axis machine tools used for five-axis machining operations. In this paper, we present a comprehensive procedure for the calibration of the rotary table including: geometric error model; error compensation method for the CNC controller; error measurement method; and verification of the error model and compensation algorithm with experimental apparatus. The methods developed were verified by various experiments, showing the validity and effectiveness of the presented methods, indicating they can be used for multi-axis machine tools as a means of calibration and precision enhancement of the rotary table.

Keywords: Ball table; Error compensation; Five-axis machine tools; Machine calibration; On-machine inspection; Rotary table; Volumetric error

1. Introduction

The industrial demand for manufacturing geometrically complex parts often calls for multi-axis machine tools to have a tool orientation capability. A rotary table (or rotary-tilting table) is often used on multi-axis machine tools as a means for providing rotational motion and is now widely used in the machine shop. Figure 1 shows a typical rotary table interfaced with a three-axis CNC machine tool [1]. The accuracy of the rotary table is crucial for part manufacturing with multi-axis machine tools. This paper is concerned with the calibration of a rotary table interfaced with a three-axis machine tool.

Many researchers have investigated the geometric error for the 3 linear axes of a machine tool from a variety of points of view. Nawara et al. [2], Soons et al. [3] and Suh et al. [4] formulated the geometric error of the machine tools from 21 error components, and proposed a prediction and compensation algorithm for the geometric errors. Ferreira and Liu [5] investigated an error modelling method for compensating errors in a three-axis machine tool. Mou and Liu [6] developed a quadratic error model based on rigid-body kinematics to enhance the precision of on-machine inspection. However, a generalised volumetric error model, describing the effects of each error component of each axis on the cutting tool position, cannot be derived from their model, owing to the complexity of representing the interaction effect between the error components. Cho et al. [7] presented a volumetric error model and applied it in precision machining of free formed surfaces. Fan et al. [8] investigated the effect of temperature on the volumetric error of machine tools, and proposed methods for their measurement and compensation. Shin et al. [9] suggested 7 tests for the characterisation of CNC machining centres.

Only a few research results were reported for rotary tables. Knapp [10] proposed a test method to measure the performance based on a rotational movement of the spindle. Although this method is simple and efficient, allowing continuous measurement, pure rotational error cannot be extracted. This is due to the fact that the volumetric error of the linear carriage is

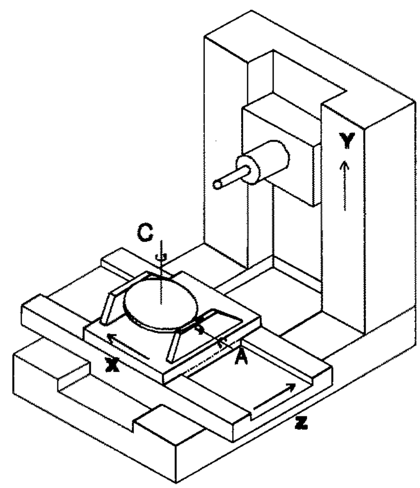

Fig. 1. Horizontal five-axis machining centre.

Correspondence and offprint requests to: Dr S.-H. Suh, Department of Industrial Engineering, Pohang University of Science and Technology, San 31, Hyoja-dong Nam-ku, Pohang, 790-784 Korea. E-mail: shs@vision.postech.ac.kr. http://camlab.postech.ac.kr

associated with the spindle movement during the test. Coorevits et al. [11] tried to reduce the geometric error of a rotary table interfaced with a three-axis machine tool, as a fourth axis. Their method is, in essence, a permutation method requiring numerous measurements to obtain reliable results. Furthermore, they did not cover all the error components of the rotary table. Recent studies [12,13] showed that the number of experimental data can be reduced by a neural network technique. By this method, they compensated only for positioning errors for a single linear motion, not for the 3D error vectors.

In this paper, we present a comprehensive procedure for the calibration of a rotary table including:

1. A geometric error model using a homogeneous transform matrix.
2. An error compensation method for CNC control.
3. An experimental procedure for error measurement and verification.

An on-machine measurement method using a ball table was developed for verification.

2. Error Model of the Rotary Table

In a typical five-axis machine tool configuration, as shown in Fig. 1, the rotary table provides two degrees-of-freedom of motion for the orientation of the workpiece. The two axes are denoted by *C* and *A*. In this configuration, the error vector of the tool position (including orientation) is composed of errors due to the three linear axes and the two rotational axes:

$$E_p = E(X,Y,Z) + E(C,A) \quad (1)$$

In the past, volumetric error models for $E(X,Y,Z)$ have been studied by many researchers including ourselves [4]. In this paper, we are concerned with the error modelling of the two rotational axes; $E(C,A)$. First, consider the error model for the rotational axis with respect to the *Z*-axis. In general, there exist 6 error components for a rotating axis (Fig. 2); three translation errors (L_x,L_y,L_z), two rotational errors (R_x,R_y), and one angular error with respect to the rotational axis (R_z). Error components for the *A*-axis, rotating with respect to the *X*-axis, can be similarly defined. Thus, there exist a total of 12 error

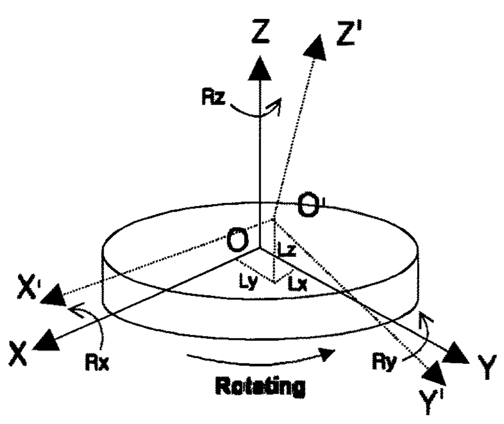

Fig. 2. Six error components for the rotary table.

components for rotary tables in the *C*- and the *A*-axes of 5-axis machine tools.

Because of the six error components, the rotary table coordinate frame is changed. Let *XYZ* be the original (or error-free) coordinate frame, and *X'Y'Z'* be the changed coordinated frame (Fig. 2). Then, the relationship between the two coordinated frames can be represented by a 4 × 4 homogeneous transform matrix. For a rotary table rotating with respect to the *Z*-axis, the transform matrix T_C can be derived as follows [14].

$$T_C(\theta_z) = \begin{bmatrix} CR_yCR_z & -CR_ySR_z & SR_y & L_x \\ SR_xSR_yCR_z + CR_xSR_z & CR_xCR_z - SR_xSR_ySR_z & -SR_xCR_y & L_y \\ -CR_xSR_yCR_z + SR_xSR_z & SR_xCR_z + CR_xSR_ySR_z & CR_xCR_y & L_z \\ 0 & 0 & 0 & 1 \end{bmatrix} \quad (2)$$

where $C = \cos$, $S = \sin$. Note that R_a in the above means $R_a(\theta_z)$ as it is varied over the angular position of the rotary table.

Applying a small angle approximation ($\cos \epsilon \approx 1$, $\sin \epsilon \approx \epsilon$), and ignoring the second-order terms, such as R_xR_y, Eq. (2) becomes Eq. (3). Similarly, the error transformation matrix for the *A*-axis; $T_A(\theta_x)$ can be derived as Eq. (4).

$$T_C(\theta_z) = \begin{bmatrix} 1 & -R_z(\theta_z) & R_y(\theta_z) & L_x(\theta_z) \\ R_z(\theta_z) & 1 & -R_x(\theta_z) & L_y(\theta_z) \\ -R_y(\theta_z) & R_x(\theta_z) & 1 & L_z(\theta_z) \\ 0 & 0 & 0 & 1 \end{bmatrix} \quad (3)$$

$$T_A(\theta_x) = \begin{bmatrix} 1 & -R_z(\theta_x) & R_y(\theta_x) & L_x(\theta_x) \\ R_z(\theta_x) & 1 & -R_x(\theta_x) & L_y(\theta_x) \\ -R_y(\theta_x) & R_x(\theta_x) & 1 & L_z(\theta_x) \\ 0 & 0 & 0 & 1 \end{bmatrix} \quad (4)$$

Owing to the error components, the actual angular position is not the same as the commanded (or nominal) angular position. As for the volumetric positioning error due to the linear axes, the magnitude of the error is not constant, but varies with angular position. In general, the error vector at θ is $P'(\theta) - P(\theta)$, where P and P' are, respectively, the commanded and the actual angular position vector. Using the transformation between the two coordinate frames, the error vector $E(\theta_z)$ can be expressed as follows:

$$E(\theta_z) = [e_x,e_y,e_z,1]^T = T_C(\theta_z)P - P \quad (5)$$

Extending this for two rotational movements, the error vector $E(\theta_z,\theta_x)$ can be derived as follows:

$$E(C,A) = E(\theta_z,\theta_x) = [e_x,e_y,e_z,1]^T = T_C(\theta_z)\, T_A(\theta_x)P - P \quad (6)$$

3. Compensation of Rotary Table Error

Because of the 12 error components, we showed that the actual position deviates from the commanded position by $E(C,A)$. The requirement is that the commanded angular position (P) should

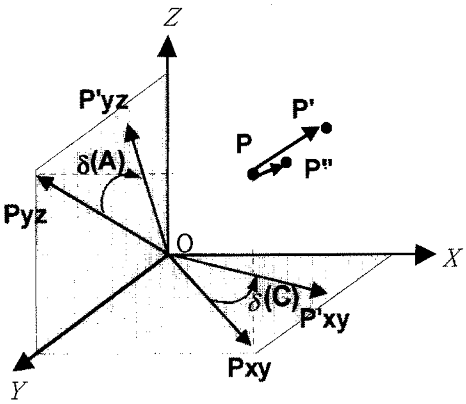

Fig. 3. Compensation of rotary table error.

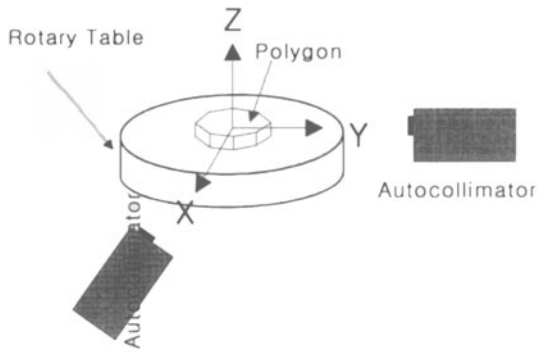

Fig. 4. Schematic view of experimental set-up for finding angular errors.

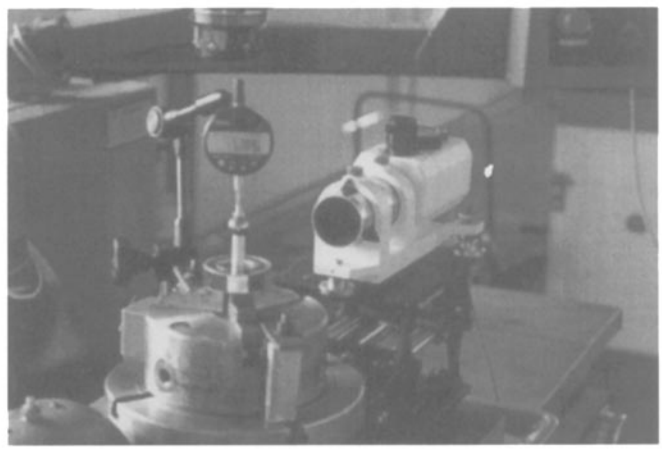

Fig. 5. Pictorial view of experimental set-up for finding errors.

be changed in some fashion so that the actual position coincides with the commanded (intended) position. In what follows, we present a compensation method for the command positions of θ_Z and θ_X.

Let $P_{a,b}$ and $P'_{a,b}$ be the projection of P and P' on the a,b plane (Fig. 3). Then, the compensated position P'' can be determined if $\delta(C)$ and $\delta(A)$ are found, where $\delta(C)$ and $\delta(A)$ are the angle between P and P' on the X, Y- and Y, Z-plane, respectively. The procedure consists of 6 steps.

1. Read in a nominal position $= [X,Y,Z,C,A] = [0,0,0,\theta_z,\theta_x]$.
2. Find $P' = T_C(\theta_z)\ T_A(\theta_x)\ P$.
3. Compute $\delta(C)$ and $\delta(A)$, defined as $\delta(C) = \angle(P_{xy},O,P'_{xy})$, and $\delta(A) = \angle(P_{yz},O,P'_{yz})$.
4. Determine $P'' = T_C(\theta_z - \delta(C))\ T_A(\theta_x - \delta(A))\ P'$.
5. Find the residual vector $\epsilon = [\epsilon_x,\epsilon_y,\epsilon_z] = P'' - P$.
6. If $|\epsilon| \leq tolerance$, exit. Otherwise; return compensated position $= [X,Y,Z,C,A] = [-\epsilon_x,-\epsilon_y,-\epsilon_z,\theta_z - \delta(C),\theta_x - \delta(A)]$.

It is worth noting that the above angular compensation algorithm yields positional correction (ϵ) as well as angular compensation. This is due to the fact that the change of rotational angle accompanies positional change. For the compensation of five-axis CL-data, the amount of positional correction must be incorporated into the volumetric error compensation algorithm for the linear axes (X,Y,Z). In other words, our strategy for compensating five-axis CL-data is to compensate for the two angular coordinates, followed by compensation for the three Cartesian coordinates.

4. Measurement of Rotary Table Errors

To obtain a complete error model for the rotary table, the error components should be measured. In this section, the measurement method is developed based on the BS 3800 scheme [15], followed by actual experiments. In what follows, we confine our discussion to the C-axis rotary table.

4.1 Measurement of Rotational Errors

For measuring the three rotational errors (R_x,R_y,R_z) of the rotary table, our method is to use a polygon mirror attached on the rotary table together with two autocollimators as shown in Fig. 4. A photograph of our experimental set-up is shown in Fig. 5. The polygon mirror has 12 faces at every 30° around the periphery, and autocollimator is set up in two directions; the X-direction for measuring the R_z and R_y errors, and the Y-direction for the R_z and R_x errors.

The two measured R_z errors must be the same. It is not required to set the polygon in the centre of the rotary table, as long as the autocollimater beam is directing on the face of the polygon mirror throughout the entire rotation. In general, the measurement values are dependent on the direction of rotation, and hence average values should be taken.

Figure 6 shows the measurement results for R_x,R_y,R_z. They are average values of three experiments. From the results, it is clear that:

1. Rotational errors for X and Y are sinusoidal.
2. The rotating direction does not much affect the amount of error for R_x and R_y.

For R_z, however,

3. The rotating direction is significant.
4. The bandwidth for the same direction is relatively constant (less than 10 s).

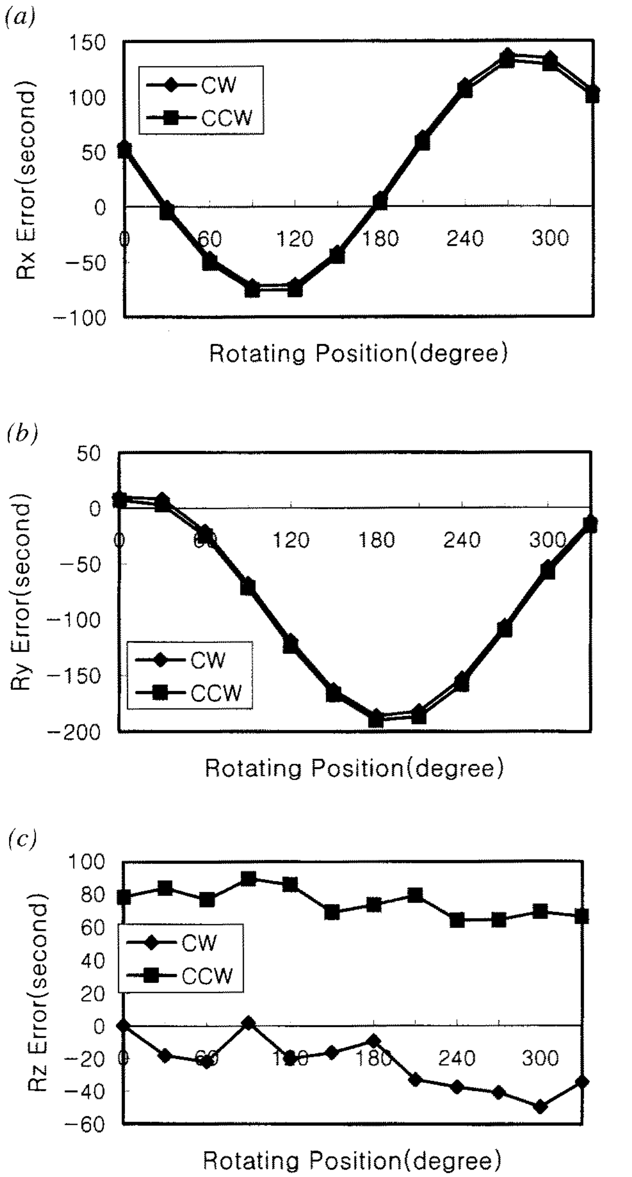

Fig. 6. Experimental results of angular errors. (*a*) R_x, *x*-direction error. (*b*) R_y, *y*-direction error. (*c*) R_z, *z*-direction error.

Overall, the rotary table we measured showed significant rotational errors, especially for rotations with respect to the *X*- and the *Y*-axis.

4.2 Measurement of Translational Errors

To measure three translation errors (L_x,L_y,L_z) of the rotary table coordinate frame, a master ball and three LVDTs (1 μm resolution) with flat tips were used. The high precision master ball, made of tungsten carbide (roundness less than 0.1 μm), was set on the centre of the rotary table as shown in Fig. 7 (photograph in Fig. 5). The LVDTs were set to zero at the starting position, then the displacements of the centre of the master ball were measured every 30°.

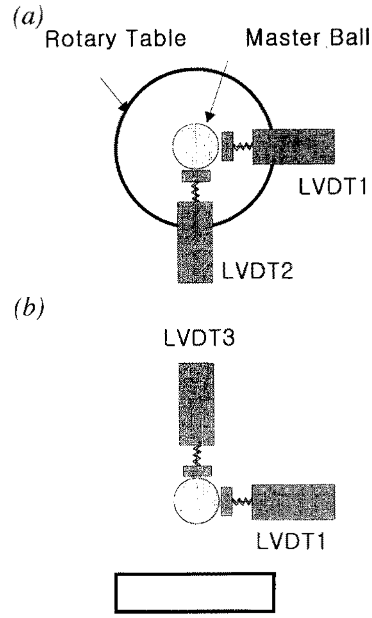

Fig. 7. Experimental set-up for finding translational errors. (*a*) on the *x*, *y*-plane, (*b*) on the *x*, *z*-plane.

Suppose *M*-plots were obtained by plotting $\{M_x^i, M_y^i, M_z^i, i \in [1:12]\}$, the measured data from the three LVDTs. In the ideal case when the position of the centre of the master ball does not change throughout the rotation, all the values will be the same, yielding a straight line parallel to the horizontal axis for the angular position. Otherwise, the *M*-plots will deviate (fluctuate) from the reference line, which can be thought of as the change of position of the master ball centre. If the master ball is precisely positioned on the centre of the rotary table, then the deviation becomes the translation error of the rotary table. In practice, however, other errors (namely set-up errors) are unavoidable, owing to the imperfect positioning of the master ball (the details will be given below). Thus, to obtain a more precise translation error, the set-up errors should be eliminated from the measured data.

Suppose that the centre of the master ball deviates from the rotary table centre, then the locus of the ball centre will be an eccentric circle (on the *X*,*Y*-plane) as the rotary table rotates (with the assumption that the rotational centre of the rotary table is fixed). This phenomenon will result in a sine curve form of the *M*-plots. The centre of the eccentric circle can be obtained by computing the centre of the LMS (least mean square) circle formed by the *M*-plots. Thus, the procedure for finding (L_x^i, L_y^i, L_z^i) is as follows:

1. Read in $\{M_x^i, M_y^i, M_z^i, i \in [1:12]\}$.
2. Construct the LMS sphere and find the centre of the LMS sphere.
3. Convert the centre coordinate values into *M*-plots.
4. To obtain $\{L_a^i, M_a^i, a = X,Y,Z, i \in [1:12]\}$ subtract the converted centre coordinates from $\{M_a^i, a = X,Y,Z, i \in [1:12]\}$.

Before showing the experimental results, it is worth analysing the set-up errors. Theoretically, there are two types of set-up error; one due to the eccentric setting of the ball; i.e.

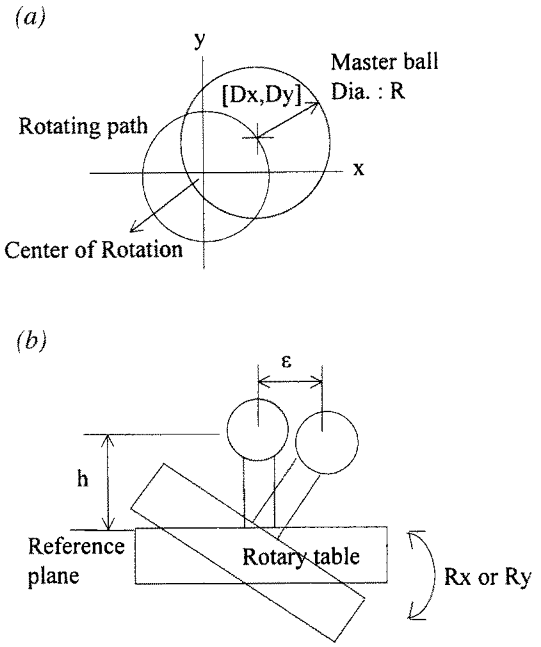

Fig. 8. Set-up errors of the master ball. (*a*) eccentric error, $[D_x, D_y]$ on the x,y-plane, (*b*) eccentric error, ϵ, due to the master ball stem h.

eccentric error (D_x,D_y) in the x,y-plane (Fig. 8(*a*)), and the other due to the reeling motion of the rotary table, i.e. eccentric error (ϵ) in the x,z- or y,z-plane (Fig. 8(*b*)). The eccentric errors (D_x,D_y) are due to the imperfect set-up of the table centre, which varies with the angular position of the rotary table. The second type of eccentric error is due to the tilting motion (R_x or R_y) of the rotary table, which can be expressed as follows:

$$\begin{bmatrix} \epsilon_x \\ \epsilon_y \end{bmatrix} = \begin{bmatrix} h \sin R_y \\ -h \sin R_x \end{bmatrix} \quad (7)$$

where h is the distance between the reference plane and the centre of master ball. Note that ϵ is changed by the height of the reference plane, and it should be adjusted in such a way that $|\epsilon|$ is a minimum. Then, the measured data (M_x,M_y) can be related to (L_x,L_y) as follows:

$$\begin{bmatrix} L_x \\ L_y \end{bmatrix} = \begin{bmatrix} M_x - D_y - \epsilon_x \\ M_y - D_y - \epsilon_y \end{bmatrix} \quad (8)$$

The experimental results are as follows. First, we obtained the M-data by the three LVDTs for every 30°, i.e. a total of 12 data for each rotational direction, and three replications were made. Figure 9 gives M-plots obtained in this way. Applying the set-up error elimination procedure, the L-plots shown in Fig. 10 were obtained. Comparing the two figures, it is clear that:

1. The set-up error was present in the raw data (M-plots).
2. The set-up error elimination procedure did reduce the translation errors significantly.

From Figs 10(*a*) and 10(*b*), we observed that:

1. The translational errors take a sine or cosine form for L_x and L_y.

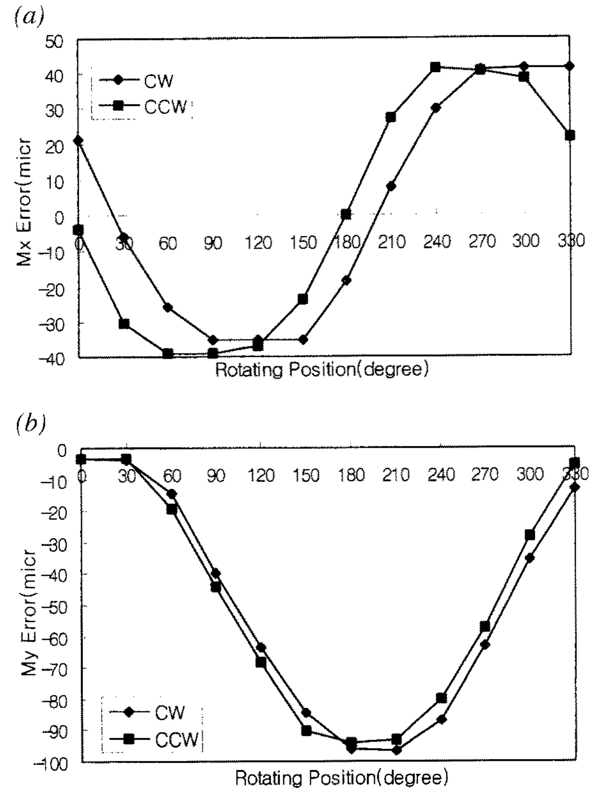

Fig. 9. M-plots including set-up errors. (*a*) x-directional translation error, M_x. (*b*) y-directional translation error, M_y.

2. The directional effect due to backlash is not significant (within 10 μm even for L_x having the largest backlash).

From Fig. 10(*c*):

4. L_z is constant throughout the settings.
5. The directional effect is not significant within 5 μm.

Based on the above, the following conclusion can be drawn:

1. The translational errors are very systematic, indicating that calibration is crucial for enhancing the precision of a rotary table.
2. Translation errors for the X- and Y-directions are significant (± 0.2 mm).
3. Translation errors are not significant for the Z-direction within 5 μm.

It is worth mentioning that the source of the positioning error of the rotary table was the non-circularity of the rollers, the straightness of the guide way and the clearance between the upper plate stem and the base hall of the rotary table as shown in Fig. 11. This explains why the positional deviation in the horizontal direction (L_x,L_y) is significant compared with that in the vertical direction error (L_z).

5. Experimental Verification

After finding the error components of the rotary table, we attempted to test the validity of the rotary table error model

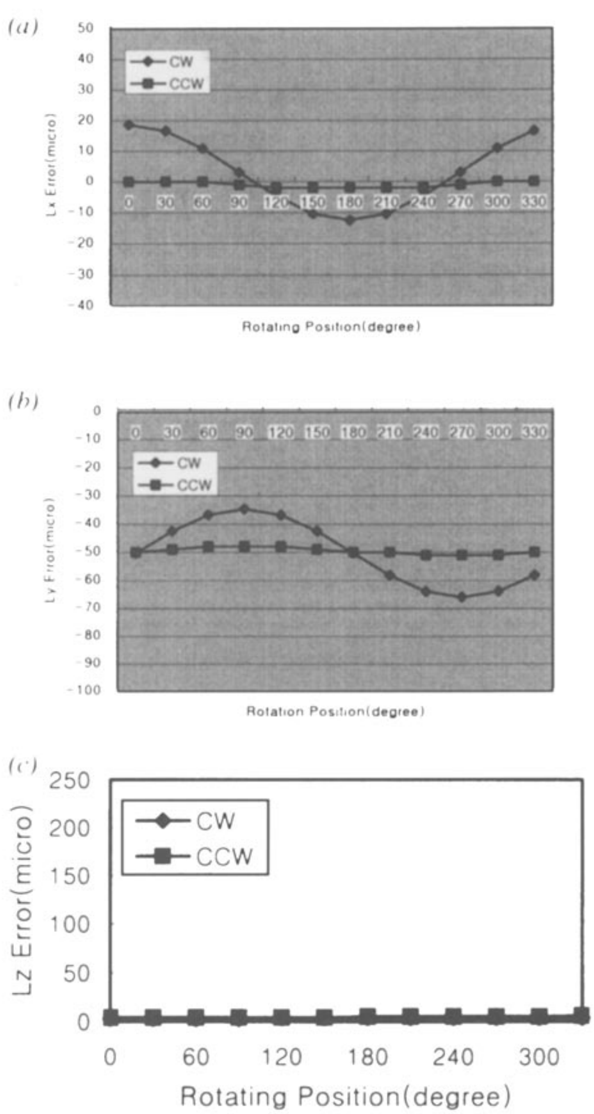

Fig. 10. Experimental results of translational errors. (*a*) *x*-direction error, L_x. (*b*) *y*-direction error, L_y. (*c*) *z*-direction error, L_z.

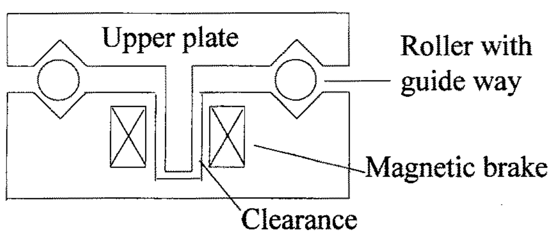

Fig. 11. Structure of rotary table.

(given in Section 2) together with the compensation algorithm (given in Section 3). For such a purpose, a ball table was designed and manufactured as shown in Fig. 12, and a touch probe was attached on the machine spindle (see photograph in Fig. 13). On the ball table, 12 precision master balls were glued onto the cone-shaped holes so that two-thirds of the ball protruded above

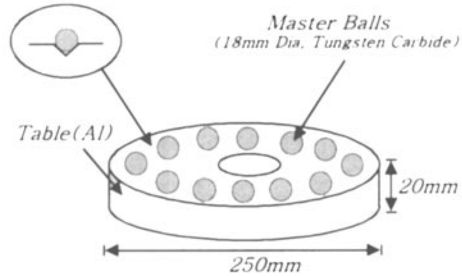

Fig. 12. Manufactured ball table.

the ball table. In the real experiment explained below, however, we used only one ball, called the *reference* ball. The distances from the ball table centre to the balls were precisely calibrated using a CMM, and the calibrated ball table was set on the rotary table in such a way that the centre of the ball table is precisely aligned with the rotational axis of the rotary table. In practice, however, perfect alignment cannot be made by any means. In our experiment, we aligned the two axes very closely by trial-and-error. As mentioned in the concluding remarks, this is a potential source of error in the verification accuracy.

5.1 Calibration of the Ball Table with the CNC Controller

The experimental procedure begins with the calibration procedure. The purpose of calibration is to align the ball table coordinate frame with that of the CNC controller. The calibration procedure is:

1. Finding the centre of the ball table (this is done by the touch probe by measuring several points around the hole surface of the ball table).
2. Moving the machine bed to the centre point found in 1.
3. Followed by resetting the CNC coordinates.

In this way, the centre of the ball table is (0,0,0) in the CNC controller. The next step is to align the reference ball (one of the twelve balls) with the *C*-axis of the CNC coordinate in a similar way. Without loss of generality, in what follows, we assume that the CNC coordinate of the reference master ball

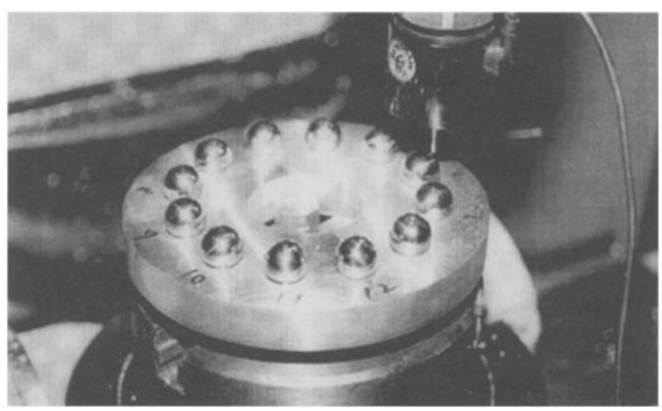

Fig. 13. The set-up for the verification experiment.

is $(a,0,0,0,0)$, where a is the distance between the reference master ball centre and the ball table centre.

5.2 Verification Method

Recall that we have two missions in this experiment:

1. To verify the error model given in Section 2.
2. To verify the compensation algorithm given in Section 3.

Suppose the ball table is rotated by 30° by sending the command (0,0,0,30,0) to the CNC controller, followed by moving the machine table (by jogging) until the probe touches the reference ball (Fig. 13). Then, record the CNC coordinate. Repeating the same procedure for the other surface points of the reference ball, the centre coordinates of the reference ball can be obtained by computing the centre of the circle with the measured coordinates. This can be repeated for the rest of the rotary table position; $\theta_z = 60, 90, \ldots, 360$.

Let the coordinates obtained be $P^*(\theta_z = 30i,\ i \in [1:12])$. To find the accuracy of the error model, one would compare the measured position with the computed position, $P' = T_C(\theta_z = 30i)[a,0,0,1]^T$, meaning that the modelling error $E_{\text{model}} = P^* - P'$, However, this is not correct, owing to the fact that the measured coordinates include the volumetric error of the linear carriage as follows:

$$P^*(\theta_z = 30i) = P(\theta_z = 30i) + E(X,Y,Z) + \epsilon \quad (9)$$

where P is the true position, $E(XYZ)$ is the volumetric error of the linear carriage, and ϵ is the random error. To avoid the above problem, $E(P^*)$ should be subtracted from P^*. In this case, the modelling error $E_{\text{model}} = P^* - E(P^*) - P'$. Note that the volumetric error at P^* ($E(P^*)$) can be computed using the algorithm given in [4]. In the real experiment, however, we did not employ this method as we were concerned with the calibration of the rotational motion, which is the purpose of this paper. In what follows, an alternative method avoiding delving into the volumetric errors is illustrated.

Consider a procedure for verifying the compensation algorithm. To test the validity, we need two positions to compare:

1. $P^*(\theta_z = 30i)$ (measured coordinate of the reference ball centre with NC command of $[0,0,0,30i,0]$).
2. P^* (*compensated_coordinate_i*) (measured coordinate of the reference ball centre with compensated NC command of $[-\epsilon_x^i, -\epsilon_y^i, -\epsilon_z^i, 30i - \delta^i(C), -\delta^i(A)]$. (this is from Step 6 of the compensation algorithm in Section 3).

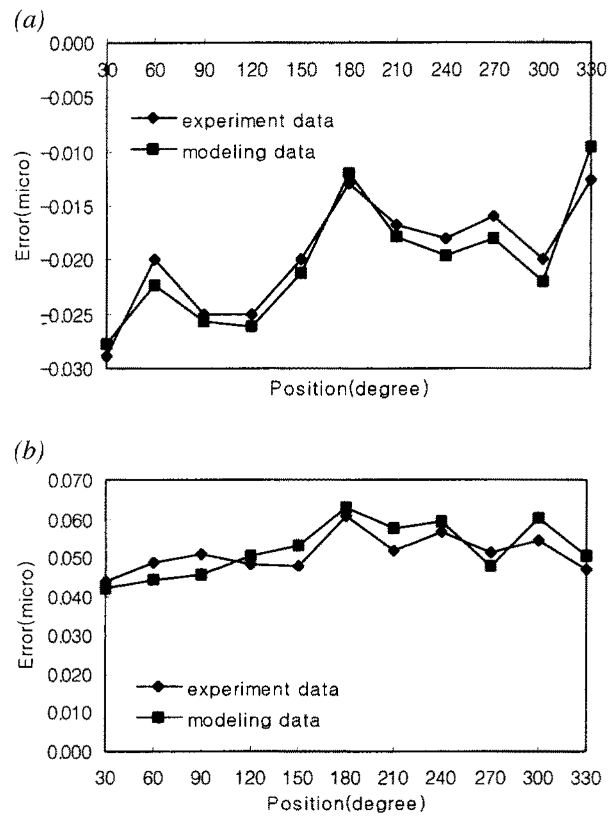

Fig. 14. Comparison of modelling and experimental data. (*a*) *x*-directional error. (*b*) *y*-directional error.

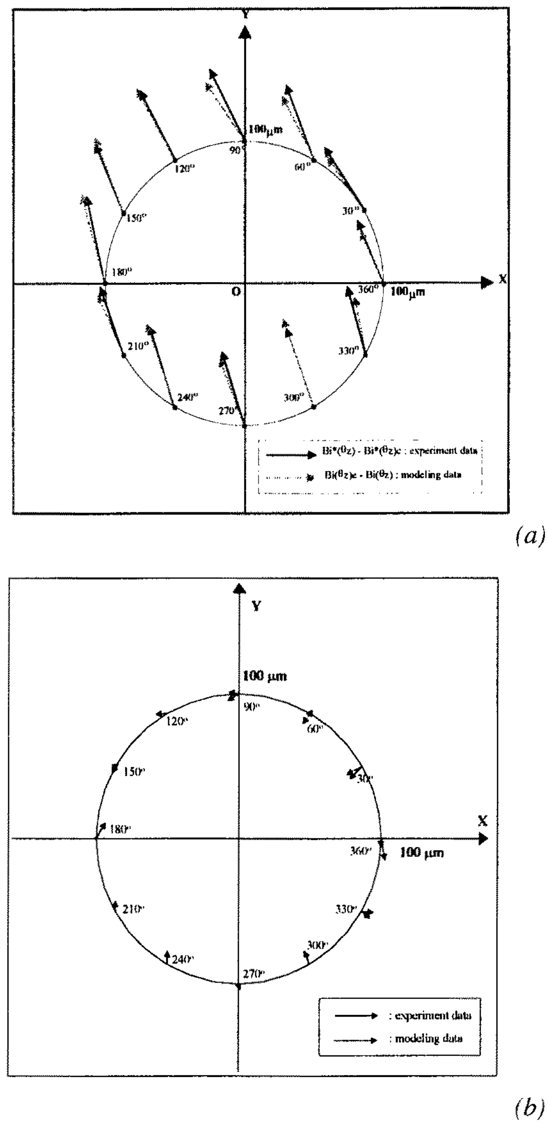

Fig. 15. Error comparison on the *x*,*y*-plane. (*a*) without compensating eccentric error. (*b*) after compensating eccentric error.

It should be pointed out that both P^* ($\theta_z = 30i$) and P^* (*compensated_coordinate_i*) contain volumetric errors.

Assuming that the volumetric error differences at the two positions are negligible (this is a fair assumption since the two positions would be very close), the positional difference between $P^*(\theta_z = 30i)$ and P^* (*compensated_coordinate_i*) is mainly due to the rotary table error:

$$P^*(\theta_z = 30i) - P^* \ (compensated\_coordinate\_i) = \text{Rotary table error} + \epsilon \quad (10)$$

where ϵ is the random error.

In terms of modelling, the rotary table error can be computed by comparing the following two positions:

$$P(\theta_z = 30i) - P'(\theta_z = 30i) = \text{Rotary table error} \quad (11)$$

where $P(\theta_z = 30° = Rot[Z,\theta_z(30i)] \in R^{4\times4}$, and $P'(\theta_z = 30i) = T_C(\theta_z = 30i)\ [a,0,0,1]^T$.

Therefore, our strategy for the two missions is to compare the measured rotary table error of Eq. (10) with the computed rotary table error of Eq. (11). If the two are very close, we can conclude that both the error modelling and the compensation methods are valid.

5.3 Experimental Results

Figure 14 shows the experimental results for 12 angular positions in *X*- and *Y*-components. The errors for the "experimental data" and "modelling error" are, respectively, based on Eqs (10) and (11). Note that we did not experiment in the *Z*-direction since the compensation for the *Z*-direction was not meaningful as observed in Fig. 10(*c*). The experimental data were obtained by averaging the measurement data in the clockwise and counterclockwise directions. Figure 14 shows that the modelling and experimental data are very close (within 5 μm), indicating the validity of the error model and compensation method. Through the analysis, it was shown that the eccentric error of the rotary table centre was less than 5 μm after compensation. The same data were plotted in two dimensions in Fig. 15(*a*). Removing the eccentric error of the rotary table, the difference between the two data sets was reduced, as shown in Fig. 15(*b*).

6. Concluding Remarks

In this paper, we addressed the error of rotary table attached to multi-axis CNC machine tools. An error model was formulated in homogeneous transformation matrix form, followed by error compensation. Then, the procedure for finding the error components was developed together with experimental apparatus. Through experimental tests, the method presented for error modelling and the error finding methods together with the compensation method were validated. Through experimental analysis, the set-up error elimination procedure, and the verification methodology were found to be effective.

However, a possible misalignment of the rotational axis of the ball table with that of the rotary table in the verification procedure could be source of inaccuracy. Considering that perfect alignment in practice cannot be guaranteed by any means, several trial-and-error attempts should be made to obtain close alignment. Nevertheless, the various experimental results convinced us that the methods presented can be used as a means for the maintenance of, the calibration of, and the precision enhancement for a rotary table on the multi-axis machine tool. Including the above problem, combined error modelling to deal with the five axes simultaneously and development of a five-axis CL-data compensation algorithm for precision machining of free formed surfaces are left for further study.

References

1. S. Suh and J. Lee, "5-axis part machining with 3-axis CNC machine tools and rotary table", ASME Transactions Journal of Manufacturing Science and Engineering, 120, pp. 120–128, 1998.
2. L. Nawara, M. Kowalski and J. Sladek, "The influence of kinematic errors on the profile shapes by means of CMM", Annals of CIRP, 38(1), pp. 511–516, 1989.
3. J. Soons, F. Theuws and P. Schllekens, "Modeling the errors of multi-axis machines: a general methodology", Precision Engineering, 14(1), pp. 5–19, 1992.
4. E. Lee, S. Suh and J. Shon, "A comprehensive method for calibration of volumetric positioning accuracy of CNC-machines", International Journal of Advanced Manufacturing Technology, 14, pp. 43–49, 1998.
5. P. Ferreira and C. Liu, "An analytical quadratic model for the geometric errors of a machine tool", Journal of Manufacturing Systems, 5(1), pp. 51–63, 1989.
6. J. Mou and C. Liu, "A method for enhancing the accuracy of CNC machine tools for on-machine inspection", Journal of Manufacturing Systems, 11(4), pp. 29–237, 1995.
7. J. Cho, M. Cho and K. Kim, "Volumetric error analysis of a multi-axis machine tool machining a sculptured workpiece", International Journal of Production Research, 32(2), pp. 345–363, 1994.
8. K. Fan, J. Lin and S. Lu, "Measurement and compensation of thermal error on a machining center", Proceedings of the Fourth International Conference on Automatic Technology, Hsinchu, Taiwan, pp. 261–268, 8–11 July 1996.
9. Y. Shin, H. Chin and M. Brink, "Characterization of CNC machining centers", Journal of Manufacturing Systems, 10(5), pp. 407–421, 1991.
10. W. Knapp, "Testing rotary axes on maching tools", Annals of CIRP, 39(1), pp. 549–552, 1990.
11. T. Coorevits, J. David and E. Lille, "Elimination of geometrical errors by permutations – applications to a rotary table", Annals of CIRP, 40(1), pp. 531–534, 1991.
12. S. Veldhuis and M.m. Elbestawi, "A strategy for the compensation of errors in five-axis machining", Annals of CIRP, 44(1), pp. 373-377, 1995.
13. J. Ziegert and P. Kalle, "Error compensation in machine tools: a neural network approach", Journal of Intelligent Manufacturing, 5, pp. 143–151, 1994.
14. A. Slocum, Precision Machine Design, Prentice Hall, Englewood Cliffs, New Jersey, 1992.
15. General Tests for Machine Tools, BS 3800 Part 2, 1991.